Early expression of capsule during Bacillus anthracis germination

Solène Fastenackels, Michèle Mock, Jean-Nicolas Tournier, Pierre L Goossens

Early expression of capsule during *Bacillus anthracis* germination

Solène Fastenackels, Michèle Mock, Jean-Nicolas Tournier, Pierre L. Goossens

PII: S0923-2508(23)00029-3

DOI: https://doi.org/10.1016/j.resmic.2023.104054

Reference: RESMIC 104054

To appear in: *Research in Microbiology*

Received Date: 28 October 2022

Revised Date: 10 March 2023

Accepted Date: 15 March 2023

Please cite this article as: S. Fastenackels, M. Mock, J.-N. Tournier, P.L. Goossens, Early expression of capsule during *Bacillus anthracis* germination, *Research in Microbiologoy*, https://doi.org/10.1016/j.resmic.2023.104054.

Early expression of capsule during *Bacillus anthracis* germination

Solène Fastenackels[a], Michèle Mock[b] , Jean-Nicolas Tournier[c], Pierre L. Goossens[d]*

Affiliations :

[a] Laboratory "Immune Microenvironment and Immunotherapy", INSERM U1135, Centre d'Immunologie et des Maladies Infectieuses Paris (CIMI-Paris), Paris, France

[b] Institut Pasteur, c/o Yersinia Unit, 26 rue du Docteur Roux, 75724 Paris cedex 15

[c] IRBA, Div.DNRBC/D.2MI, 1, place Général Valérie André, 91223 Brétigny/Orge

[d] Institut Pasteur, Yersinia Unit, 26 rue du Docteur Roux, 75724 Paris cedex 15

[a] solene.fastenackels@sorbonne-universite.fr

[b] michele.mock@pasteur.fr

[c] jntournier@gmail.com

[d]* pierre.goossens@pasteur.fr Correspondance and reprints

Abstract

Bacillus anthracis is a spore-forming bacterium that produces two major virulence factors, a tripartite toxin with two enzymatic toxic activities and a pseudo-proteic capsule. One of the main described functions of the poly-gamma-D-glutamate capsule is to enable *B. anthracis* bacilli to escape phagocytosis. Thus, kinetics of expression of the capsule filaments at the surface of the emerging bacillus during germination is an important step for the protection of the nascent bacilli. In this study, through immunofluorescence and electron microscopic approaches, we show the emergence of the capsule through a significant surface of the exosporium in the vast majority of the germinating spores, with co-detection of BclA and capsular material. This suggests that, due to an early capsule expression, the extracellular life of *B. anthracis* might occur earlier than previously thought, once germination is triggered. This raises the prospect that an anti-capsular vaccine may play a protective role at the initial stage of infection by opsonisation of the nascent encapsulated bacilli before their emergence from the exosporium.

Keywords

Bacillus anthracis; spore; capsule; germination

1. Introduction

The virulence of *Bacillus anthracis*, the etiological agent of anthrax, relies predominantly on two main factors, a tripartite toxin with two enzymatic activities (lethal and edema factors, metalloprotease and adenylcyclase activities respectively) and a pseudoproteic capsule made of poly-gamma-D-Glutamic acid (PDGA)[1] The capsule protects the bacteria from phagocytosis, is poorly immunogenic [2] and potentially disruptive for the immune response [3, 4]; it enables the bacteria to bind to the liver endothelium [5] and plays a role in sequestration inside pulmonary capillaries at the terminal phase of the infection [6].

B. anthracis is a spore-forming bacterium. The spore is a specialised cell form that remains dormant and survives for many years, formed of concentric shells surrounding the core that contains the bacterial genetic material: a membrane: a peptidoglycan layer - the cortex: a protein multilayer –the coat: and the exosporium –the outermost structure of the spore [7-9]. The exosporium is composed of a basal layer and an external hair-like nap formed by a single collagen-like glycoprotein called BclA [10, 11]). Upon germination there is an influx of water into the spore, swelling of the spore core, dismantling of the cortex and coat leading to resumption of metabolic activity and cell growth [7-9].

Early expression of the toxin genes has been shown [12], as soon as 15 min after germination triggering for mRNA detection. This suggests a potential early role for them in subverting the host defense. Temporal expression of the capsule is also critical to enable protection of the nascent bacilli. How the capsule emerges from a germinating spore that is surrounded by the exosporium and the coat layers is thus of importance.

In this study, we addressed the kinetics of capsule expression during *B. anthracis* germination. We observed early detection of capsular material as soon as 15 min after germination triggering. Capsular material was detected in the majority of spores as emerging all around the external layers of the spore.

2. Materials and methods

2.1 Bacterial growth

The *B. anthracis* strains used were the encapsulated non-toxinogenic RPG1 strain derived from the RPLC2 strain after transduction of the pXO2 of the ATCC 4229 strain [13], the parental non-encapsulated RPLC2 strain [14] and the Δ-*bclA* RPG1-derived strain (constructed as described previously [10]); the RPLC2 strain is derived from the Sterne strain with one point mutation in the *lef* gene and two point mutations in the *cya* gene leading to enzymatically inactive toxins. To synchronise spore germination, spores (1×10^7 mL -1) were shortly incubated in BHI for 3 min at 37° [13] . This incubation step triggered germination in more than 90% of the spores, allowing the analysis of a homogeneous germinating spore population, as germination was less efficiently triggered in the minimum culture R-medium. After centrifugation (13,000 rpm, 2 min), the germinating spores were resuspended in R-medium with 0.6% sodium bicarbonate [15] and incubated at 37 °C in a 5% CO_2 atmosphere; this growth condition mimics the *in vivo* environment and ensures coordinated *in vitro* expression of the capsule and the toxins. At various timepoints, bacteria were collected, washed in Dulbecco′s Phosphate Buffered Saline with $MgCl_2$ and $CaCl_2$ (Sigma, ref D8662) and then analysed by immunofluorescence or ultrastructural studies (see below).

For the *in vivo* approach, 1×10^8 germinated spores obtained after the BHI incubation step were injected intraperiteonally in female outbred Swiss OF1 mice (weight, 22–24 g; Charles River, L'Arbresle, France). One hour later, the animals were euthanasised, a peritoneal lavage was performed with 10 mL cold Dulbecco′s Phosphate Buffered Saline without $MgCl_2$ and $CaCl_2$ (Sigma, ref D8537) ; the suspension of bacterial and peritoneal cells were then centrifuged in PBS with $MgCl_2$ and $CaCl_2$ (1200rpm, 5 min) to pellet the majority of peritoneal cells, the supernatant was then centrifuged (4000rpm, 8mn) to pellet the bacterial suspension. After resuspension in PBS with $MgCl_2$ and $CaCl_2$, the bacteria were processed for immuno-staining. Animals were housed in the Institut Pasteur animal facilities, licensed by the French Ministry of Agriculture and in compliance with European regulations. All animal experiments were conducted according to European Union guidelines https://ec.europa.eu/environment/chemicals/lab_animals/3r/ key_resources/portals_en.htm and were approved by the animal care and use committee at the Institut Pasteur.

2.2 Immunofluorescence and ultrastructural studies

The germinated spores were fixed in 4% paraformaldehyde for 15 min, deposited on poly-L-lysine-coated (PLL) glass coverslips as described previously [16]. In brief, coverslips were sequentially incubated for 1 hour at room temperature with appropriate dilutions of the primary antibodies and of the species-specific secondary fluorochrome conjugates in PBS 0.25% gelatin. Each incubation was followed by three washes of 10 minutes with PBS. In some experiments, the host cell nuclei were stained with 100 nM Topro-3 in the Vectashield mounting medium.

The exosporium protein BclA was detected with the mouse monoclonal antibody 4B7G12 developed in the laboratory, revealed by an Alexa488-labelled donkey anti-mouse secondary polyclonal antiserum. For the exosporium of the Δ-*bclA* RPG1 strain, devoid of the BclA protein, primary labelling was performed with a murine polyclonal anti-exosporium antiserum raised against Δ-*bclA* spores developed in the laboratory.

The PDGA capsular material was detected with a polyclonal rabbit immune serum revealed by an Alexa594-labelled goat anti-rabbit polyclonal antiserum as previously described [17]. No cross reaction between the various antibodies was observed (data not shown). Confocal microscopy was performed on a Leica SP5 confocal microscope using a 63x, oil immersion objective. Image deconvolution was performed as already described [18].

Quantification of the spore populations exhibiting distinct patterns of BclA and PGDA-labelling was performed at various times of the germination kinetics and the vegetative cells were excluded (Table 1).

Transmission electron microscopy was performed on dendritic cells (DC) at 1h of infection with RPG1 and RPLC2 spores as previously described [19]. In brief, DC were infected with the spores and analysed after 30 min. Cells were fixed for 3 h in 3% glutaraldehyde in 0.1 M phosphate buffer and postfixed for 1 h with 1% OsO4 in 0.1 M cacodylate buffer. The pellet was embedded in epoxy resin and sectioned for transmission electron microscopy.

Scanning electron microscopy was performed on 45 min-germinated spores bound to PLL-coated coverslips; after overnight fixation in 2.5 % glutaraldehyde in 0.1 M sodium cacodylate buffer at 4 °C, and incubation with 1/100 diluted in BHI (brain heart infusion) anti-PDGA specific rabbit polyclonal antibodies and anti-BclA mouse monoclonal antibodies as described above and then incubated with a 15 nm immuno-gold conjugate (British Biocell International) coupled with an anti-rabbit goat antibody, and of 10 nm immuno-gold conjugate (British Biocell International) coupled with an anti-mouse goat antibody. Finally, a negative staining was performed with phosphotungstic acid 2 % in water.

Of note, all image acquisitions were carried out on PLL-coated supports. This originated from the observation that carbon-coated grids preferentially bound spores that do not present capsular material at the surface in contrast to PLL-coated grids. Indeed, only 5 % of the spore population was positive for anti-capsular material labelling on carbon-coated grids versus 61 % for the PLL-coated grids, as assessed through immunofluorescence detection as described above. Such approach is thus critical to avoid misrepresentation of a particular subpopulation.

3. Results

The presence of PDGA capsular material and the BclA protein - an abundant protein of the spore surface - was detected through immuno-fluorescence labelling with specific antibodies (Fig. 1&2); quantitative analysis of both fluorescence signal topographic distribution was performed on the samples (Table 1 built on kinetics as shown in Fig. 1&2).

At 30 and 45 min (Fig. 1), many germinating spores of the encapsulated RPG1 strain were labelled with both anti-capsular material and anti-BclA antibodies; co-detection of capsular material and BclA was observed around the whole, or greater part of, spore surface, in 67 % of the bacterial population at 30 min (forms 5+6 in Table 1). This proportion for the forms 5+6 was still around 57 % at 60 min (Table 1); at this timepoint, 29 % of the bacterial cells (form 8 in Table 1) were labelled as encapsulated bacteria that were devoid of anti-BclA labelling. This population (form 8 in Table 1) increased, as expected, to reach 76 % of the labelled bacteria at 120 min, with a few remnants of anti-BclA labelled exosporium; the remaining bacterial cells were anti-BclA labelled spores that did not undergo the germination step (Fig. 1 and form 1 in Table 1). Interestingly, a particular topographic distribution of fluorescence was observed in 8 % of the germinating spores at 30 min; capsular material was observed as dots on some locations of the BclA layer (form 2 in Table 1).

Triple labelling (Topro-3 for DNA, and anti-BclA and anti-capsular material labelling) was performed at 45 min, at a time point when the majority of the germinating spores were labelled for BclA and capsule (Fig. 1, time point 45 min); all germinating spores harboured DNA and thus were not empty exosporium shells. Using mouse anti-exosporium polyclonal antibodies, similar co-detection of capsular material and the exosporium layer at 45 min was also observed with spores from a strain deleted of the *bclA* gene (Fig 1).

Raising the question of the timepoint of initial detection of the anti-capsular material labelling, we observed that capsular material could be detected as early as 15 min of incubation in R medium 0.6% sodium bicarbonate in a 5% CO_2 atmosphere (Fig 2). Quantitatively, this fluorescence signal was detected in 60% of the germinating spores (forms 4+5+6 in Table1). No capsular material labelling was detected immediately after the 3min-germination step in BHI, while all spores were labelled with the anti-BclA antibody (Table 1 and Fig. 2).

To confirm that this phenomenon also occurs *in vivo*, the germinated spores were inoculated in mice into the peritoneum cavity and bacterial growth allowed to develop *in vivo*; the bacterial cells were recovered after 1h of growth and immunolabelled as above (Fig. 1,

uttermost right panel). Similar co-detection of capsular material and BclA around the bacterial surface was observed.

Analysis of the fluorescent images at 30 and 45 min suggested that the capsular material was detected outside the BclA layer (Fig. 1). To analyse this particular aspect in more detail, two complementary approaches were developed, confocal microscopy and image deconvolution (Fig. 3a top and bottom panels respectively). Both approaches strongly suggested the capsular material was localised outside the BclA layer. Image deconvolution also suggested that the capsular material was distributed as dots around the surface (Fig. 3a bottom panel).

To confirm this observation, an ultrastructural approach was followed, through electron microscopy (Fig 3b and c). Transmission electron microscopy without labelling showed deposition of electron dense material as dots around the most external surface of the encapsulated germinating RPG1 spores inside the hair-like BclA layer (Fig 3b, left), while this was not observed with the parental non-encapsulated RPLC2 strain (Fig 3b, right).

We then used a specific qualitative analysis through scanning electron microscopy with labelling by immunogold co-detection of antibodies directed against capsular material (15 nm beads) and BclA (10 nm beads). We were able to observe spores that presented small packs of labelled capsular material that emerge in various locations of the labelled exosporium (Fig. 3c).

4. Discussion

In this study, we addressed the kinetics of capsule expression and topographic distribution during germination of *B. anthracis* spores, using immunofluorescence and electron microscopy approaches. We show co-detection of both antigens peaking at 30-45 min after germination triggering.

Topographically, the capsular material was detected in the majority of the germinating spores around the whole surface of the exosporium. This strongly suggests that the external spore layers were fissured and the capsular material synthesised by the nascent bacilli emerged through these fissures and breaks. Indeed, dots of capsular material could be detected around the BclA layer in 8% of the germinating spores at 30 min (form 2 in Table 1). This phenomenon was also observed for *in vivo* infection.

Our data thus strongly suggest that *B. anthracis* behaves similarly to *B. atrophaeus* and *B. subtilis*, where fissures and breaks have been observed in the coat during germination. [20, 21]. Interestingly, John Ezzell reported a similar finding many years ago [22]; this observation was exploited as a means for *B. anthracis* spore identification through this phenomenon of 'spore encapsulation'. Of note, we could also observe bacterial cells where the nascent bacillus emerged from the spore coat and exosporium layers only at one end, leaving behind an empty shell. This was in accordance with previously published data reporting that, during spore germination and outgrowth, the outgrowing cell escapes from its exosporium shell by popping through a region of the exosporium that could not be stained by antibodies to the spore specific alanine racemase [23].

Toxins and capsule are expressed in a coordinated manner, at the genetic and molecular levels [24, 25]. Our study shows that capsular material could be detected as soon as 15 min. PA mRNA has been reported as early as 15 min after germination, thus highlighting the precocity of toxin production [26]. Similarly, lethal and edema factors were detected in the plasma of mice as early as one hour after intranasal inoculation [27]. Two consequences of this early capsular material expression and distribution on the surface of the germinating spores may be envisioned.

(i) The lifestyle of *B. anthracis*, an extracellular pathogen, at this early stage is considered to follow two different initial scenarios at the portal of entry into the infected host - an extracellular or an intracellular step - the physiological importance of each one depending on the route of entry. On one hand, during a cutaneous infection, *B. anthracis* spores germinate very efficiently in the extracellular tissues [28].Furthermore, as reported in inhalational and gastrointestinal infections, as soon as a lesion is present, efficient spore

germination occurs at the lesion site [29]. On the other hand, an intracellular pathway has been described, playing a role in the crossing of the respiratory or intestinal epithelial barriers during inhalational and gastrointestinal infections [30-32]; spores are engulfed and, through trafficking, emerge from the cells on the other side of the epithelium. Our study thus suggests that, in both scenarios, early expression of capsular material around the germinating spore would help protect the emerging nascent bacilli at a crucial timepoint when *B. anthracis* is susceptible to the host innate defenses, as it is converting from the resistant dormant spore to the virulent toxinogenic encapsulated bacillus. Combined with early expression of toxins [26, 27] this would help subvert the host defenses.

(ii) a second outcome of such early capsular material expression on the germinating spores is that they may become a target for a pre-existing anti-capsular vaccine immune response. Current veterinary vaccines rely on live attenuated spores of the toxinogenic non-encapsulated Sterne strain, while human vaccines are mainly based on the common toxin component protective antigen (PA) [33]. However these PA-based vaccines for human use are protective only in some specific animal models [34]. To enhance their efficacy, other components have been added experimentally, especially for protection against inhalational anthrax. Addition of inactivated spores as a source of spore antigens notably increases the efficiency of an anthrax vaccine in the mouse model [14, 35]. Addition of spore or bacilli components, or more specifically of capsular material, have been considered and tested [17, 36, 37]; in particular, the group of Arthur Friedlander has further demonstrated the role of anti-capsule immunity in vaccine development [38, 39]. Our data suggest that the approaches of adjoining capsular material to the current anthrax human vaccines would thus be beneficial earlier than considered; opsonisation of the nascent encapsulated bacilli, even before emergence from the exosporium, would play a protective role at the initial stage of infection.

Acknowledgments

We would like to express our thanks to Tam Mignot for the deconvolution analysis, Evelyne Tosi-Couture (Pasteur Institute) and Guy Brochier (IRBA) for their expertise in ultrastructural analysis, and Jean-Philippe Corre for his contributions and discussions.

Conflict of interest

All authors have no conflict of interest

References

[1] Mock M, Fouet A. Anthrax. Annual review of microbiology 2001;55:647-71.

[2] Fouet A. The surface of *Bacillus anthracis*. Molecular aspects of medicine 2009;30:374-85.

[3] Jelacic TM, Ribot WJ, Chua J, Boyer AE, Woolfitt AR, Barr JR, et al. Human Innate Immune Cells Respond Differentially to Poly-gamma-Glutamic Acid Polymers from *Bacillus anthracis* and Nonpathogenic Bacillus Species. J Immunol 2020;204:1263-73.

[4] Jelacic TM, Ribot WJ, Tobery SA, Chabot DJ, Friedlander AM. Poly-gamma-Glutamic Acid Encapsulation of *Bacillus anthracis* Inhibits Human Dendritic Cell Responses. ImmunoHorizons 2021;5:81-9.

[5] Piris-Gimenez A, Corre JP, Jouvion G, Candela T, Khun H, Goossens PL. Encapsulated *Bacillus anthracis* interacts closely with liver endothelium. The Journal of infectious diseases 2009;200:1381-9.

[6] Jouvion G, Corre JP, Khun H, Moya-Nilges M, Roux P, Latroche C, et al. Physical Sequestration of *Bacillus anthracis* in the Pulmonary Capillaries in Terminal Infection. The Journal of infectious diseases 2016;214:281-7.

[7] Driks A. The *Bacillus anthracis* spore. Molecular aspects of medicine 2009;30:368-73.

[8] Moir A. How do spores germinate? Journal of applied microbiology 2006;101:526-30.

[9] Setlow P. Spore germination. Current opinion in microbiology 2003;6:550-6.

[10] Sylvestre P, Couture-Tosi E, Mock M. A collagen-like surface glycoprotein is a structural component of the *Bacillus anthracis* exosporium. Molecular microbiology 2002;45:169-78.

[11] Sylvestre P, Couture-Tosi E, Mock M. Polymorphism in the collagen-like region of the *Bacillus anthracis* BclA protein leads to variation in exosporium filament length. Journal of bacteriology 2003;185:1555-63.

[12] Cote CK, Welkos SL. Anthrax Toxins in Context of *Bacillus anthracis* Spores and Spore Germination. Toxins 2015;7:3167-78.

[13] Gimenez AP, Wu YZ, Paya M, Delclaux C, Touqui L, Goossens PL. High bactericidal efficiency of type IIa phospholipase A2 against *Bacillus anthracis* and inhibition of its secretion by the lethal toxin. J Immunol 2004;173:521-30.

[14] Brossier F, Levy M, Mock M. Anthrax spores make an essential contribution to vaccine efficacy. Infection and immunity 2002;70:661-4.

[15] Ristroph JD, Ivins BE. Elaboration of *Bacillus anthracis* antigens in a new, defined culture medium. Infection and immunity 1983;39:483-6.

[16] Prina E, Abdi SZ, Lebastard M, Perret E, Winter N, Antoine JC. Dendritic cells as host cells for the promastigote and amastigote stages of *Leishmania amazonensis*: the role of opsonins in parasite uptake and dendritic cell maturation. Journal of cell science 2004;117:315-25.

[17] Candela T, Dumetz F, Tosi-Couture E, Mock M, Goossens PL, Fouet A. Cell-wall preparation containing poly-gamma-D-glutamate covalently linked to peptidoglycan, a straightforward extractable molecule, protects mice against experimental anthrax infection. Vaccine 2012;31:171-5.

[18] Mignot T, Merlie JP, Jr., Zusman DR. Regulated pole-to-pole oscillations of a bacterial gliding motility protein. Science (New York, N.Y 2005;310:855-7.

[19] Tournier JN, Quesnel-Hellmann A, Mathieu J, Montecucco C, Tang WJ, Mock M, et al. Anthrax edema toxin cooperates with lethal toxin to impair cytokine secretion during infection of dendritic cells. J Immunol 2005;174:4934-41.

[20] Plomp M, Leighton TJ, Wheeler KE, Hill HD, Malkin AJ. In vitro high-resolution structural dynamics of single germinating bacterial spores. Proceedings of the National Academy of Sciences of the United States of America 2007;104:9644-9.

[21] Santo LY, Doi RH. Ultrastructural analysis during germination and outgrowth of *Bacillus subtilis* spores. Journal of bacteriology 1974;120:475-81.

[22] Ezzell JW, Abshire TG. Encapsulation of *Bacillus anthracis* spores and spore identification. Salisbury Medical Bulletin 1996;87S:42.

[23] Steichen CT, Kearney JF, Turnbough CL, Jr. Non-uniform assembly of the *Bacillus anthracis* exosporium and a bottle cap model for spore germination and outgrowth. Molecular microbiology 2007;64:359-67.

[24] Fouet A, Mock M. Regulatory networks for virulence and persistence of *Bacillus anthracis*. Current opinion in microbiology 2006;9:160-6.

[25] Koehler TM. *Bacillus anthracis* physiology and genetics. Molecular aspects of medicine 2009;30:386-96.

[26] Cote CK, Rossi CA, Kang AS, Morrow PR, Lee JS, Welkos SL. The detection of protective antigen (PA) associated with spores of *Bacillus anthracis* and the effects of anti-PA antibodies on spore germination and macrophage interactions. Microbial pathogenesis 2005;38:209-25.

[27] Rougeaux C, Becher F, Goossens PL, Tournier JN. Very Early Blood Diffusion of the Active Lethal and Edema Factors of *Bacillus anthracis* After Intranasal Infection. The Journal of infectious diseases 2020;221:660-7.
[28] Corre JP, Piris-Gimenez A, Moya-Nilges M, Jouvion G, Fouet A, Glomski IJ, et al. In vivo germination of *Bacillus anthracis* spores during murine cutaneous infection. The Journal of infectious diseases 2013;207:450-7.
[29] Glomski IJ, Piris-Gimenez A, Huerre M, Mock M, Goossens PL. Primary involvement of pharynx and peyer's patch in inhalational and intestinal anthrax. PLoS pathogens 2007;3:e76.
[30] Goossens PL, Tournier JN. Crossing of the epithelial barriers by *Bacillus anthracis*: the Known and the Unknown. Frontiers in microbiology 2015;6:1122.
[31] Russell BH, Vasan R, Keene DR, Koehler TM, Xu Y. Potential dissemination of *Bacillus anthracis* utilizing human lung epithelial cells. Cellular microbiology 2008;10:945-57.
[32] Weiner ZP, Glomski IJ. Updating perspectives on the initiation of *Bacillus anthracis* growth and dissemination through its host. Infection and immunity 2012;80:1626-33.
[33] Tournier JN, Ulrich RG, Quesnel-Hellmann A, Mohamadzadeh M, Stiles BG. Anthrax, toxins and vaccines: a 125-year journey targeting *Bacillus anthracis*. Expert review of anti-infective therapy 2009;7:219-36.
[34] Goossens P. Animal models of human anthrax: The Quest for the Holy Grail. Mol Aspects Med. 2009;doi:10.1016/j.mam.2009.07.005
[35] Gauthier YP, Tournier JN, Paucod JC, Corre JP, Mock M, Goossens PL, et al. Efficacy of a vaccine based on protective antigen and killed spores against experimental inhalational anthrax. Infection and immunity 2009;77:1197-207.
[36] Friedlander AM, Little SF. Advances in the development of next-generation anthrax vaccines. Vaccine 2009;27 Suppl 4:D28-32.
[37] Manish M, Verma S, Kandari D, Kulshreshtha P, Singh S, Bhatnagar R. Anthrax prevention through vaccine and post-exposure therapy. Expert opinion on biological therapy 2020;20:1405-25.
[38] Chabot DJ, Ribot WJ, Joyce J, Cook J, Hepler R, Nahas D, et al. Protection of rhesus macaques against inhalational anthrax with a *Bacillus anthracis* capsule conjugate vaccine. Vaccine 2016;34:4012-6.
[39] Chabot DJ, Scorpio A, Tobery SA, Little SF, Norris SL, Friedlander AM. Anthrax capsule vaccine protects against experimental infection. Vaccine 2004;23:43-7.

Legends to figures

Figure 1: Co-detection of capsular material and exosporium during germination of *B. anthracis* spores of the encapsulated RPG1 strain and the *bclA*-deleted derived strain (Δ-*bclA*): germinating spores were immuno-labelled 30 and 45 min after germination triggering for 3 min in BHI and further growth in R-medium 0.6% Bicarbonate in 5% CO2 atmosphere. Representative germinating spores are represented at higher magnification beside groups of bacterial cells for each time points. Red fluorescence for anti-capsular material labelling, green fluorescence for monoclonal anti-BclA or polyclonal anti-exosporium labelling for the Δ-*bclA* strain. Simultaneous DNA labelling (Topro-3, blue fluorescence) is shown at 45 min. For the *in vivo* germinating spores, 1 x 10^8 germinated RPG1 spores obtained after the 3min-BHI incubation step were inoculated intraperitoneally and recovered one hour later. Images are representative of at least two to three experiments (except for the *in vivo* experiment for ethical reasons).

Figure 2: Kinetics, from 15 min to 2h, of co-detection of capsular material and exosporium BclA during germination of *B. anthracis* spores of the encapsulated RPG1 strain; same growth conditions and immunofluorescence labelling as in Fig.1. The 3-min time point represents the spores after germination triggering in BHI, in conditions where the capsule is not expressed.

Figure 3: Same growth conditions as in Fig.1. (a) Same immunofluorescence labelling as in Fig.1; (top) confocal analysis of germinating spores at 45 min, (bottom) image deconvolution in the same experimental conditions. (b and c) spore germination was studied independently by transmission electron microscopy w/o labelling (JNT's lab) and by scanning electron microscopy with specific labelling of BclA and capsular material (PLG's lab) - (b) Transmission electron microscopic analysis of extracellular RPG1 spores (left) and the non-encapsulated RPLC2 parental strain (right) 1h after dendritic cell infection (see Materials and methods). (c) scanning electron microscopic analysis of immunolabelled RPG1 germinating spores at 45 min (see Fig. 1) ; 10 nm beads for the anti-BclA antibodies, 15 nm beads for the anticapsular material antibodies (see Materials and methods); to facilitate reading of the image is shown in the insert a colored representation of the 10 nm anti-BclA beads (colored in green) and 15 nm anti-capsule beads (colored in red) in a representative given area of the spore.

399 **Table 1:** Quantitative analysis of the topographical distribution of the immunofluorescence
400 during germination of the encapsulated RPG1 strain; a numbered schematic representation of
401 the type of observed immunofluorescence signals is shown in the two left columns. After a
402 3min-step of germination triggering ("0"min), germinated spores were incubated in R
403 medium 0.6% bicarbonate in a 5% CO2 atmosphere, recovered at various time points
404 thereafter and immunolabelling performed after binding on PLL-coated glass coverslips (see
405 Materials and Methods). Enumeration of the labelled spores is expressed as percentage (n=
406 number of spores enumerated on successive fields). red: anticapsular material labelling, green:
407 anti-BclA labelling.
408

Form type	Immuno-fluorescence distribution	"0" min (n=103)	15 min (n=55)	30 min (n=64)	60 min (n=59)	90 min (n=50)	120 min (n=50)
1		100%	16 %	9 %	10 %	26 %	24 %
2			24 %	8 %			
3	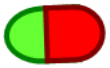			2 %			
4			31 %	12 %	3 %	4 %	
5			27 %	31 %	10 %	2 %	
6	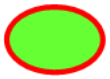		2 %	36 %	47 %	16 %	
7				2 %			
8					29 %	52 %	76 %

Table 1: Fastenackels et al

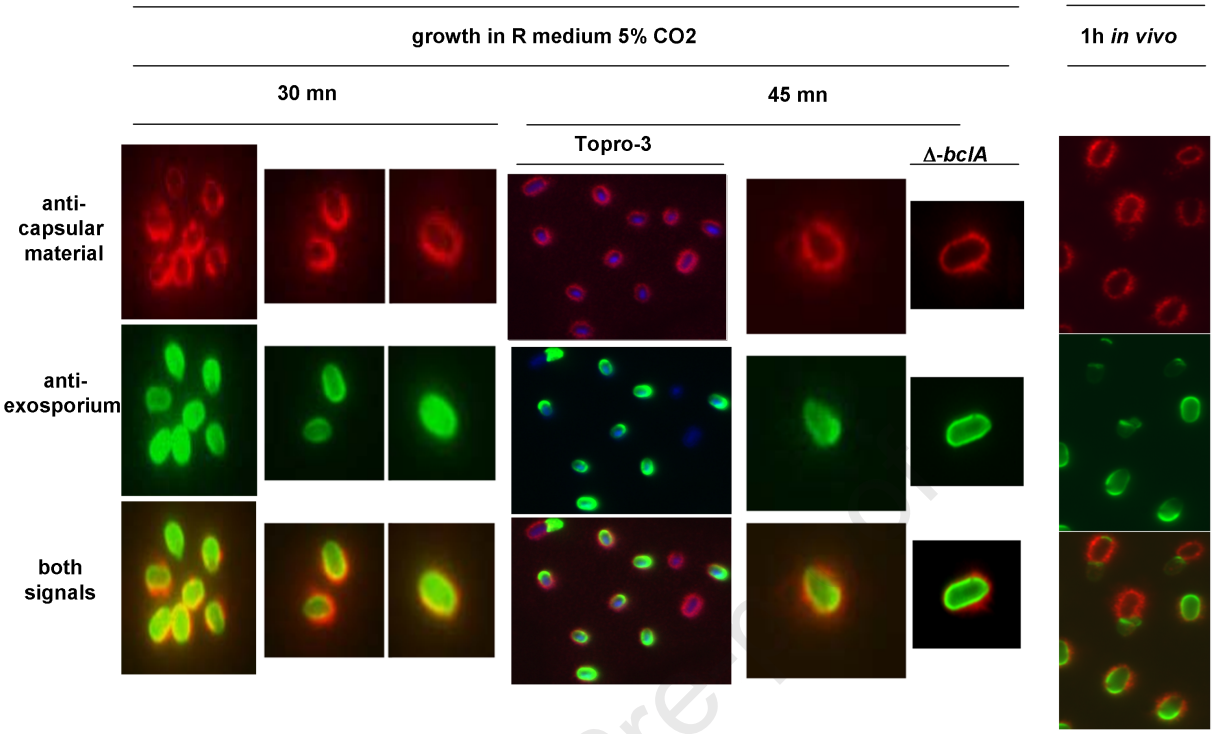

Fig 1: Fastenackels et al

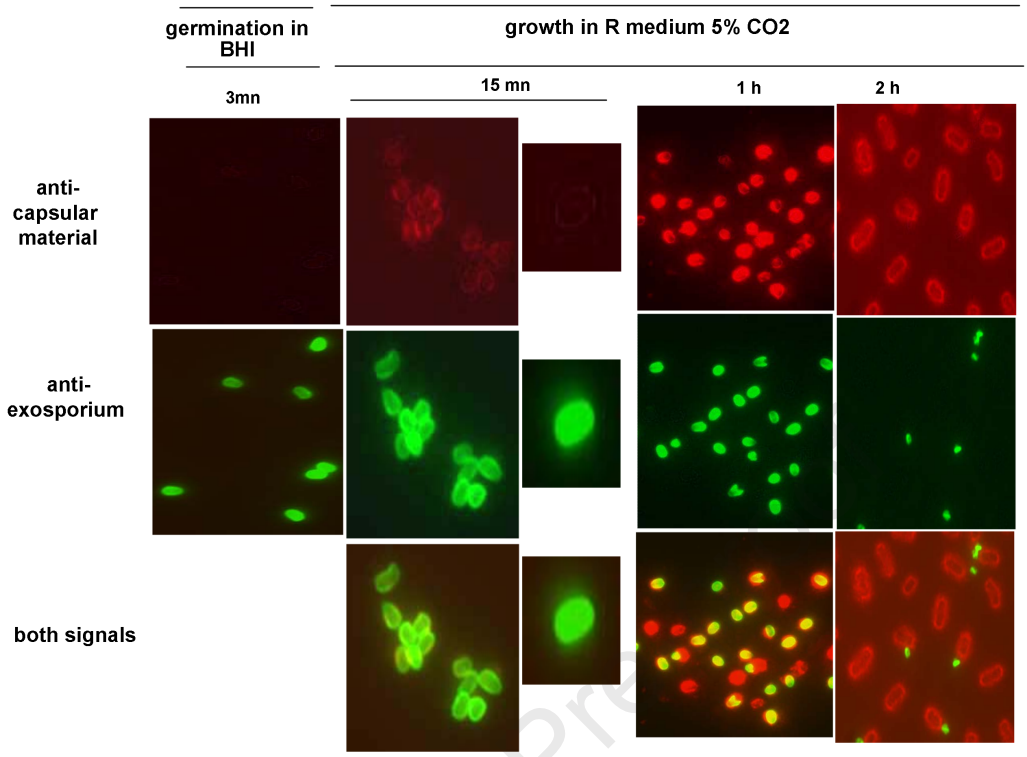

Fig 2: Fastenackels et al

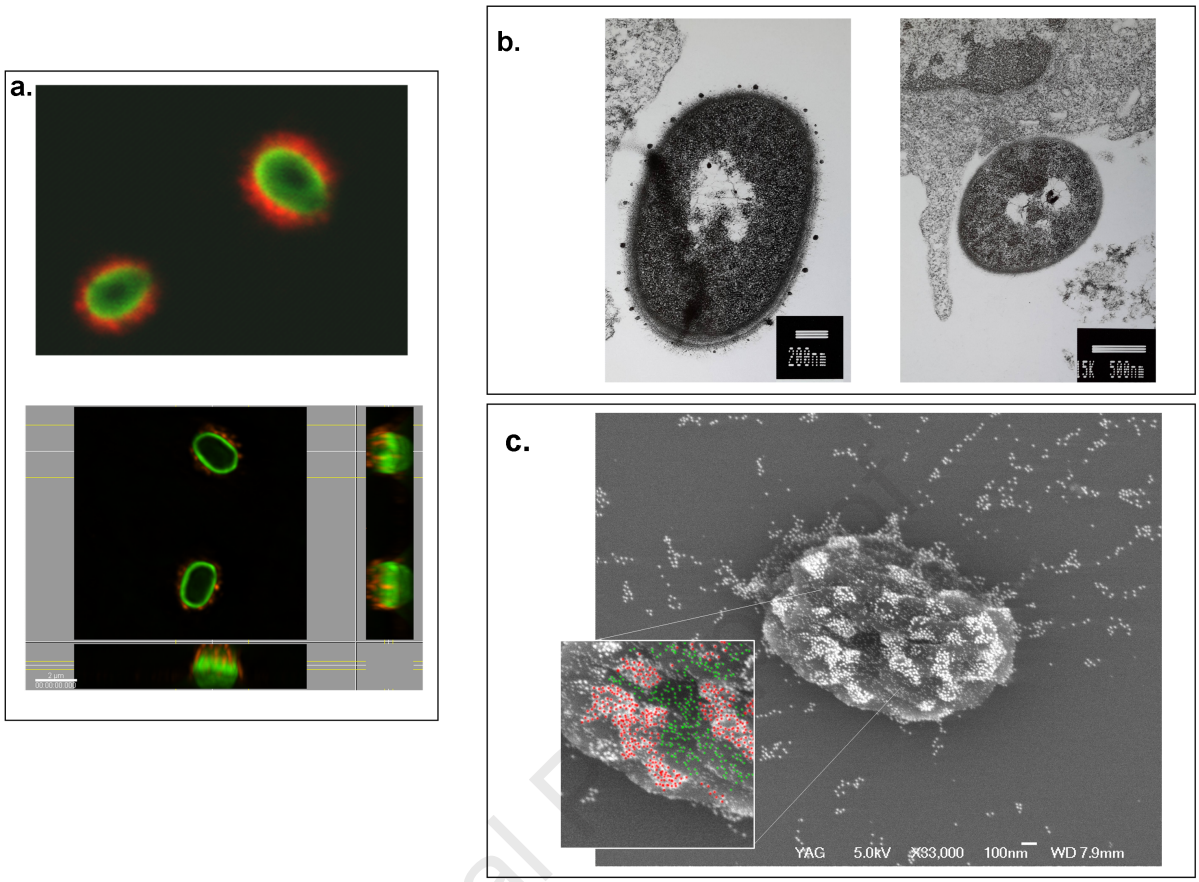

Fig 3: Fastenackels et al